Valence-band structures of phosphorus allotropes

Nancy B. Goodman,* L. Ley, and D. W. Bullett†
Max Planck Institut für Festkörperforschung, Heisenbergstrasse 1, D-7000 Stuttgart 80, Federal Republic of Germany
(Received 3 February 1983)

X-ray photoemission spectra (XPS) of several forms of phosphorus have been measured with the use of a monochromatized Al $K\alpha$ x-ray source with a resolution of ~ 0.6 eV full width at half maximum. We have investigated orthorhombic black phosphorous, cubic white phosphorus, and triclinic NaP_{15} as well as bulk amorphous red phosphorus and plasma-deposited hydrogenated amorphous thin films, and present the first published XPS spectra of most of these allotropes. We also report the results of electronic structure calculations for orthorhombic phosphorus and for the tetrahedral P_4 molecular constituent of cubic white phosphorus (w-P). Differences in densities of states are interpreted in terms of the different bonding configurations of the various allotropes. The spectra of black P is fitted well by the calculated valence bands. The spectra of amorphous P are not inconsistent with the presence of pentagonal tubes of phosphorus atoms as they are present in Hittorf's phosphorus and in NaP_{15}. The electronic structure of w-P is well described by that of isolated P_4 tetrahedra.

I. INTRODUCTION

Phosphorus was first isolated by Hennig Brand in 1669.[1] Since then it has been obtained in more allotropic modifications than any other element.[2] At present, there are over a dozen bulk solid forms known as well as several thin-film modifications. Interest has largely concentrated on the structure and chemistry of these allotropes and our knowledge about the electronic structure of phosphorus is still limited.

Fichter,[3] Fomichev,[4] Wiech,[5] and Zuckerman[6] have measured the soft x-ray emission spectra of black and red phosphorus and the first band-structure calculations of black phosphorus have recently become available.[7,8] By comparison, there is an extensive literature on the electronic structure of the other group-V elements As, Sb, and Bi both in their crystalline and amorphous forms.[9–16]

It is the purpose of this work to investigate with x-ray photoemission spectroscopy (XPS) the electronic structure of the most common forms of bulk phosphorus, namely orthorhombic black, cubic white, and amorphous red. We have also studied NaP_{15}, a polyphosphide that contains structural elements characteristic of Hittorf's phosphorus, another crystalline allotrope of phosphorus. In addition we present data on a new material, thin-film hydrogenated amorphous phosphorus (a-P:H) prepared by the plasma decomposition of phosphine. A preliminary account of the valence-band spectra of this material has been given by von Roedern *et al.*[17]

White phosphorus (w-P) has a cubic structure with 58 tetrahedral P_4 units per unit cell and is grown by condensation from P_4 vapor. The bonding within the P_4 units is covalent whereas the phosphorus tetrahedra are held together by weaker van der Waals forces.[1] White P is cream color and waxy, has a very high vapor pressure (0.181 mm Hg at room temperature) and burns upon contact with air. w-P is an insulator but no value for the fundamental gap has been determined to our knowledge.

Controlled heating of w-P above 250 °C yields bulk amorphous red phosphorus (r-P) which is thermodynamically and chemically more stable than w-P. X-ray diffraction analysis indicates that P is threefold coordinated in r-P with an average bond distance and bond angle of 2.24 Å and 102°, respectively.[18] Red phosphorus is quite stable, even in air and is a wide gap (2.5—3.0 eV) semiconductor.

Orthorhombic black phosphorus (b-P), with eight atoms per unit cell, is obtained from several other forms of phosphorus by heating under high pressure (well over 10 kbar).[19] Orthorhombic b-P is the densest and most stable form of the element under normal conditions. The atoms are arranged in double layers as indicated in Fig. 1 with three nearest neighbors at distances of 2.224 Å and 2.244 Å, respectively, within the layer and four next-nearest neighbors in adjacent layers 3.592 Å and 3.801 Å

away.[20] Although band-structure calculations for a single layer indicate a zone-center band gap of 1.3—1.8 eV, interactions between the layers reduce the gap to 0.3 eV in both the pseudopotential calculation[8] and the present atomic-orbital calculations (see Sec. IV) for the bulk material, in agreement with electrical measurements.[21—23]

Another allotrope is the crystalline red or so-called Hittorf's phosphorus (*H*-P).[24] It crystallizes from a lead-phosphorus melt in a monoclinic space group with 84 atoms per unit cell.[25] The phosphorus atoms are arranged in the form of infinite tubes with pentagonal cross section. Only one out of 21 atoms within a tube bonds to adjacent tubes which run at right angles. All P atoms are threefold coordinated with an average bond length of 2.219 Å and an average bond angle of 100.9° (Ref. 25).

Since it had been suggested by Thurn and Krebs[25] that the pentagonal tubes of *H*-P might represent the structural elements of amorphous *r*-P, we considered it necessary to obtain the photoemission spectra of *H*-P for comparison. Unfortunately crystals of *H*-P of sufficient size were not available. Thus we investigated instead the polyphosphide NaP_{15} which contains pentagonal phosphorus tubes of a kind very similar to those of *H*-P. NaP_{15} crystallizes triclinic, it is dark red, transparent, and stable in air.[26] Phosphorus atoms are arranged in the form of infinite tubes with pentagonal cross section which are divisible into P_{15} units as shown in Fig. 2(a). Out of the 15 P atoms one is twofold coordinated and bonds directly to the Na atom. All other P atoms are threefold coordinated with bond distances of 2.18 and 2.30 Å, respectively. The bond angles are between 93° and 112°. Each Na atom unites four P_{15} segments as shown in Fig. 2(b).[27]

Thin-film amorphous phosphorus can be produced in many ways. Evaporated films must be stabilized by annealing at ~280 °C and they are yellow in color.[28] It is likely that they are incompletely polymerized *w*-P. Films prepared by plasma-assisted chemical vapor transport, on the other hand, are glassy and dark red. These films contain $\lesssim 6$ at. % hydrogen.[29,30] Films similar in appearance but without hydrogen have been obtained by sputtering *r*-P in an argon atmosphere and their structure and vibrational properties have been investigated.[31] Our hydrogenated amorphous phosphorus films prepared by the glow discharge decomposition of phosphine (PH_3) are also glassy as verified by x-ray diffraction, dark red, and stable in air.

The remainder of the paper is organized as follows. After a brief description of the experimental techniques in the next section, the photoemission data are presented in Sec. III. The results of electronic structure calculations for *b*-P, a P_4 molecule, and a single layer of orthorhombic *b*-P are given in Sec. IV. The experimental valence densities of states (DOS) of the various P modifications are finally discussed in Sec. V in the light of available band-structure calculations and structural models of amorphous phosphorus.

II. EXPERIMENTAL

All sample surfaces were prepared *in situ* in the ultrahigh-vacuum system of the spectrometer to avoid contamination since photoemission measurements are only sensitive to the first ~20 Å of the sample. For the bulk samples this involved filing to remove the oxidized and/or contaminated surface layer. The surface of *w*-P sublimed, so it did not need to be filed. The measurements on *w*-P were done at −120 to −130 °C to keep the vapor pressure below 10^{-7} mbar.

The thin-film *a*-P:H samples were deposited *in situ* by the glow-discharge decomposition of phosphine (PH_3) diluted to 1.1 at. % in argon. Samples were deposited on the grounded electrode of a capa-

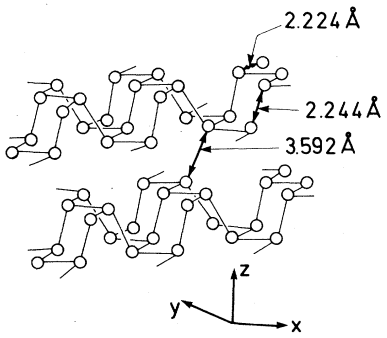

FIG. 1. Structure of black P showing portions of two infinite puckered layers. Principle interatomic distances are indicated.

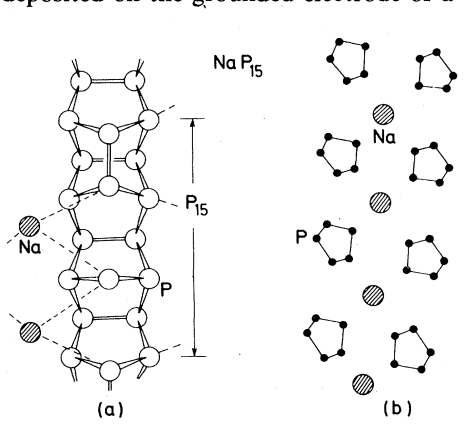

FIG. 2. Structure of NaP_{15} showing (a) portions of the infinite pentagonal phosphorus tubes and (b) the way they are arranged relative to the Na atoms.

citive system using either a dc or rf source with no noticeable effect on the spectra. Typical power was ~2 W. All parts of the system were stainless steel. The samples were deposited at room temperature. The base pressure was $\sim 5\times 10^{-8}$ mbar and the pressure was at 1.0 mbar during depositions with a flow rate of 4 SCCM (standard cc per min or 1 cm^3/min at room temperature and pressure). These films contained between 15 and 30 at. % hydrogen as estimated from the hydrogen-induced peak visible in the uv excited photoemission spectra (compare Ref. 17).

X-ray photoemission spectra were taken in a Hewlett-Packard Model 5950A ESCA spectrometer at a resolution of 0.6 eV full width half maximum (FWHM) using monochromatized Al$K\alpha$ x-rays ($h\nu = 1486.6$ eV). Measurements were made in a vacuum better than 10^{-10} mbar, except for w-P where the vacuum was determined by the vapor pressure of the sample.

Because the samples were insulating, some of them tended to acquire a (nonuniform) surface charge during the measurement. This shifted and broadened the resulting spectra. To counteract this effect we flooded the sample surfaces with low-energy electrons when necessary. The charging was especially severe for the bulk amorphous red phosphorus samples. The energy and current of the electrons were chosen to give the best resolution of the P 2p lines.

III. PHOTOELECTRON SPECTRA

For all modifications of phosphorus studied here, the binding energy of the 2p core level was 130.0±0.5 eV and that of the 2s core level 187.0±0.5 eV relative to the top of the valence bands. The line shapes and widths vary slightly with allotrope, presumably due to differences in residual charging. The spin-orbit splitting of the 2p core level was determined as (0.84±0.05) eV from a least-squares fit of the best resolved spectrum of b-P. The P 2p lines for b-P and r-P are shown in Fig. 3 as examples.

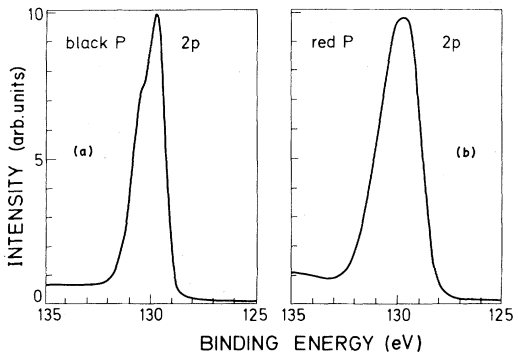

FIG. 3. Phosphorus 2p core levels for (a) orthorhombic black phosphorus and (b) amorphous red phosphorus. The energy scale is relative to the valence-band edge.

Figure 4 shows 2s and 2p core-level spectra for all types of pure phosphorus investigated. The satellites at 18—20 eV and 35—40 eV below the main peaks are energy losses due to the excitation of one or two bulk plasmons, respectively. These are marked as ω_p and $2\omega_p$. The surface plasmons at 8—10 eV below the core levels are clearest in the case of w-P because the surface was the cleanest due to its constant sublimitation. Surface plasmons, marked ω_s, are also evident as shoulders for r-P, b-P, and a-P:H in Fig. 4.

The measured plasmon energies, $(\hbar\omega_p)_{\text{expt}}$ and $(\hbar\omega_s)_{\text{expt}}$, are tabulated in Table I for the various allotropes, along with the respective densities. The plasmon frequencies are determined through $\epsilon_1(\omega_p)=0$ and $1+\epsilon_1(\omega_s)=0$, respectively, where

$$\epsilon(\omega)=\epsilon_1(\omega)+i\epsilon_2(\omega)$$

is the complex frequency-dependent macroscopic dielectric function. In the free-electron approximation of the valence electrons the Drude formula,

$$\epsilon_1(\omega)=1-4\pi n_v e^2/m\omega^2 ,$$

is valid where n_v is the density of valence electrons (proportional to the density ρ), and e and m are the electron charge and mass, respectively. From the Drude formula we calculate plasmon energies

$$(\hbar\omega_p)_{\text{calc}}=\hbar(4\pi n_v e^2/m)^{1/2}$$

and $(\hbar\omega_s)_{\text{calc}}=1/\sqrt{2}\hbar\omega_p$ which are also given in Table I. The bulk plasmon energies so obtained are somewhat *lower* than the measured ones, the largest deviation occurring in w-P where $(\hbar\omega_p)_{\text{expt}}$ exceeds $(\hbar\omega_p)_{\text{calc}}$ by 16%. From the similarity in the mea-

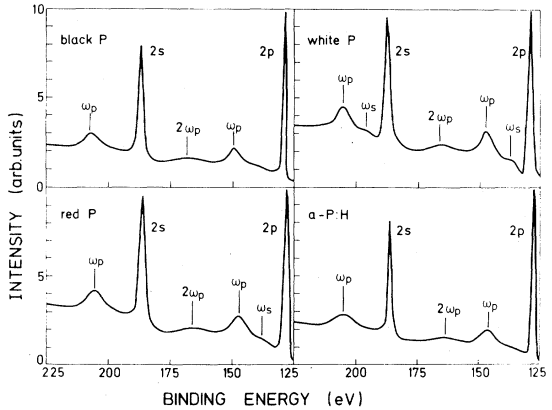

FIG. 4. XPS spectra for b-P, r-P, w-P, and a-P:H. The 2s and 2p core lines are marked. The satellites are due to the excitation bulk plasmons of energy $\hbar\omega_p$ and surface plasmons of energy $\hbar\omega_s$.

TABLE I. Bulk- and surface-plasmon energies for various modifications of P (in eV).

Allotrope	Black phosphorus	Red phosphorus	Thin-film *a*-P:H	NaP_{15}	White phosphorus
ρ(gm/cm^3)	2.69	2.16		2.377	1.83
$(\hbar\omega_p)_{\text{calc}}$[a]	19.0	17.0		17.6	15.7
$(\hbar\omega_p)_{\text{expt}}$	20.2	19.2	19.3	19.6	18.2
$(\hbar\omega_s)_{\text{calc}}$[b]	13.4	12.0	13.6[c]	12.4	11.1
$(\hbar\omega_s)_{\text{expt}}$	10.5	12.0	9.5	12.0	8.3

[a] $(\hbar\omega_p)_{\text{calc}}=\hbar(4\pi e^2 n_V/m)^{1/2}$.
[b] $(\hbar\omega_s)_{\text{calc}}=(1/\sqrt{2})(\hbar\omega_p)_{\text{calc}}$.
[c] For *a*-P:H, $(\hbar\omega_s)_{\text{calc}}=(1/\sqrt{2})(\hbar\omega_p)_{\text{expt}}$.

sured bulk plasmon energies of *r*-P and *a*-P:H we infer comparable densities of both modifications. For the surface plasmons the differences of up to 40% with the calculated energies are consistently too *high* except for *r*-P where experimental and calculated values agree.

The Drude expressions for ω_p and ω_s fail when interband transitions modify the dielectric function in the neighborhood of ω_s or ω_p. In P the interference from valence- to conduction-band transitions is apparently strong enough up to energies of ~ 10 eV to lower $\hbar\omega_s$ substantially. A similar situation is found in the neighboring Si where $(\hbar\omega_s)_{\text{expt}}$ and $(\hbar\omega_s)_{\text{calc}}$ are 8.8 and 11.7 eV, respectively.[32]

Figure 5(a) shows the raw data for the valence bands of *b*-P, in agreement with the recently published results of Harada *et al.*[33] The valence bands proper extend from ~ 2 to ~ 20 eV binding energy. One notices a replica of the valence bands above ~ 20 eV binding energy due to the plasmon losses. In order to correct for this plasmon contribution, we unfolded the valence-band spectrum using the 2*p* core-level spectrum as the response function. The resulting valence-band spectrum with the inelastic background subtracted is shown in Fig. 5(b). Because the probability for plasmon excitations depends somewhat on the kinetic energy of the electrons, the inelastic background is not expected to be identical for the valence-band and 2*p* core-level spectra for which the electron kinetic energy differs by 130 eV. This slight discrepancy leads to minor errors in the background subtraction, however, as manifested by the apparent negative intensity below 25 eV binding energy which amounts to a mere 6% of the peak height.

Valence-band spectra with inelastic backgrounds subtracted are shown in Fig. 6 for four allotropes of phosphorus. The zero of the energy scale is set to the Fermi level of the spectrometer. Owing to charging of the sample surface during measurements, this may differ from the Fermi levels of the

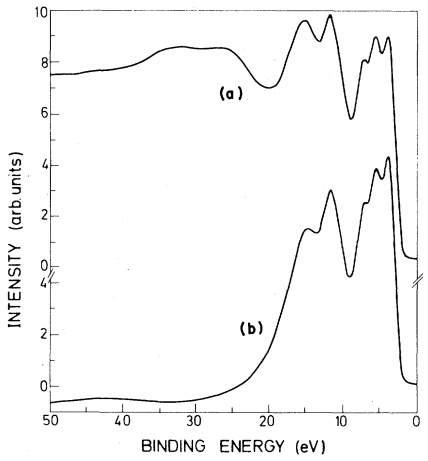

FIG. 5. Valence-band XPS spectrum of black phosphorus: (a) raw data; (b) with inelastic background subtracted.

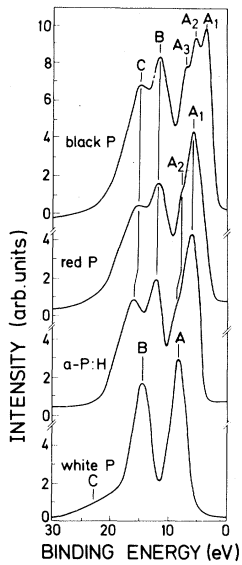

FIG. 6. Valence-band XPS spectra with inelastic background subtracted for black P, red P, *a*-P:H, and white P.

samples. In addition, the samples have band gaps ranging from ~ 0.3 to ~ 3.0 eV, so that the position of the top of the valence band relative to the bulk Fermi level may vary by as much. The uncorrected and corrected valence-band spectrum of NaP_{15} is shown in Fig. 7. The $2p$ electrons of Na produce the peak at 31.0 eV binding energy relative to the valence-band edge $E_v \equiv 0$. The Na $3s$ valence electron contributes less than 2% to the valence bands of NaP_{15} as estimated from the cross-section ratio $[\sigma(3s)]/[\sigma(2p)]=0.1$ for Na.[34] The valence-band spectrum of NaP_{15} represents thus the local density of states of the phosphorus atoms with negligible interference from the Na atoms. The same holds for the valence-band spectrum of a-P:H in Fig. 6 since the photoemission cross section for the H $1s$ states is negligible compared to that of the P $3s$ and $3p$ states at x-ray energies. Hydrogenic levels do show up in a-P:H with uv excitation as a peak 1.5 wide at a binding energy of 8.9 eV on the scale of Fig. 6.[17] The peak positions of all spectra are listed in Table II and details of the valence bands will be discussed in Sec. V.

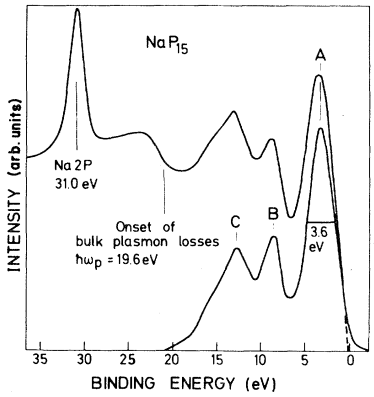

FIG. 7. Corrected and uncorrected valence-band spectrum of NaP_{15}. Zero of energy is the top of the valence bands.

IV. ELECTRONIC STRUCTURE CALCULATIONS

The electronic structures of orthorhombic black phosphorus and of white phosphorus have been calculated by the local-orbital method applied earlier to the band-structure calculations of crystalline arsenic and antimony.[10–12] The theory contains no adjustable parameters. Basis functions are the $3s$ and $3p$ atomic orbitals for phosphorus, calculated using $\alpha=0.7$ in the local-density approximation for exchange correlation. This gives atomic levels $E_{3s}=-14.7$ eV and $E_{3p}=-6.5$ eV.

In the band-structure calculations for b-P these orbitals are allowed to interact with the three nearest-neighbor atoms in the same layer (2 at 2.22 Å and 1 at 2.24 Å) and with four atoms in the adjacent layer (2 at 3.59 Å, 2 at 3.80 Å) (compare Fig. 1). The resulting band structure is shown in Fig. 8, and the corresponding density of states in Fig. 9. The spectrum divides into two asymmetric bonding and antibonding s-like peaks, centered near -13 and -17 eV in Fig. 9, a broad p-bonding feature extending from -4.4 to -10.6 eV, separated by an energy gap from the unoccupied p-antibonding states. The exact agreement between the calculated energy gap of 0.3 eV and the experimental gap in black orthorhombic phosphorus is probably coincidental—we would not expect the accuracy of the calculated bands to be better than several tenths of an eV using these approximations.

Also shown in Fig. 9 is the density of states of a single layer of b-P. Without the interlayer interactions the p-bonding band is $\sim 25\%$ narrower and the semiconducting energy gap increases to 1.3 eV.

White P is made up of tetrahedral P_4 units with 58 tetrahedra per cubic unit cell as mentioned earlier. Coupling between the P_4 units is known to be extremely weak since the barrier to rotation is low enough to allow the contribution to the heat capacity associated with the hindered rotation to approach the classical value for free rotation at the melting point.[2] We have therefore approximated the electronic structure of w-P by that of a single P_4 unit. We assumed an ideal tetrahedral arrangement of phosphorus atoms with a bond length of 2.21 Å and used the same computational procedure as for b-P.

TABLE II. Energies of peaks in the valence-band spectra of various phosphorus allotropes measured from the top of the valence bands (in eV).

Peak	Black phosphorus	Red phosphorus	a-P:H	NaP_{15}	White phosphorus
	$A1$ 1.8	$A1$ 3.6	$A1$ 3.0		
A	$A2$ 3.3	$A2$ 5.5	$A2$ 5.7	3.3	3.3
	$A3$ 4.9				
B	9.6	9.6	9.0	9.5	9.4
C	13.0	12.9	13.0	12.9	17.0

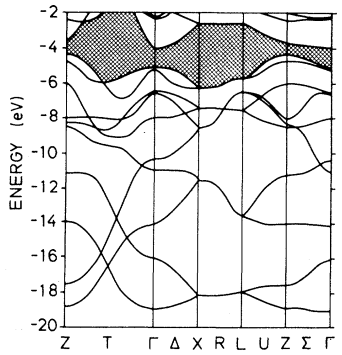

FIG. 8. Band structure of orthorhombic *b*-P calculated using the atomic-orbital method.

The resulting energy levels are listed in Table III. The occupied molecular orbitals fall into three groups: a low-lying a_1 singlet, a t_2 triplet, and the closely spaced group of six a_1, t_2, and e states. The first two groups are mainly *s*-like and the upper group mainly *p*-like. The next higher state, the unoccupied *p*-antibonding t_1 triplet, lies 4 eV higher in energy. In spite of the highly strained nature of the bonds in this molecule (with bond angles of 60° compared to $\sim 100°$ in most phosphorus allotropes) we expect the present *sp* basis to describe the bonding adequately, without the need to introduce higher *d* states in accord with the calculations of Brundle *et al.*[35] and Seifert and Grossmann.[36]

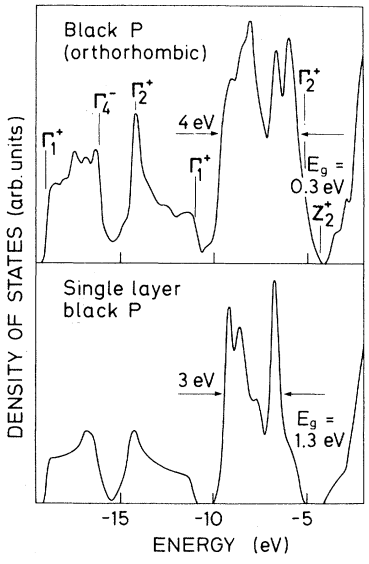

FIG. 9. Densities of states (DOS) of *b*-P and a single layer of *b*-P. The DOS's have been smoothed by folding them into a Gaussian of 0.3-eV FWHM.

TABLE III. Theoretical energy eigenvalues and orbital composition (*s* and *p*) of electronic levels in the P_4 molecule.

	Orbital	Energy (eV)	*s* (%)	*p* (%)
Empty	$7t_2$	−0.4	15	85
	$2t_1$	−2.7	0	100
Occupied	$2e$	−6.6	0	100
	$6t_2$	−7.9	8	92
	$5a_1$	−8.6	20	80
	$5t_2$	−13.6	77	23
	$4a_1$	−20.8	81	19

V. DISCUSSION

A. Orthorhombic black phosphorus

The band structure of *b*-P has been calculated by Takao *et al.*[7] using the tight-binding method (extended Hückel theory) and Asahina *et al.*[8] using the self-consistent pseudopotential approach. In both cases certain parameters were adjusted to reproduce the optical gap of 0.3 eV. The calculations give band structures and densities of states in essential agreement with those presented in the previous section for which no parameters were adjusted to obtain the optical gap of 0.3 eV. The only notable difference is the nature of the fundamental gap. It is direct at *Z* in the calculations of Asahina *et al.*[8] and Takao *et al.*[7] whereas we find an indirect gap from the valence-band maximum at *Z* to the conduction-band minimum at Γ (compare Fig. 8).

For a more quantitative comparison of the valence-band spectrum with the band-structure calculations we have chosen a number of critical points that mark the same characteristic features in the densities of states for all three calculations (compare Figs. 9 and 10). These are in order of increasing binding energy: Γ_2^+ and Γ_1^+ which define the top and bottom of the *p*-like peak in the density of states (DOS); Γ_2^+ and Γ_4^- coincide with the two *s*-like peaks ($B+C$), and finally, Γ_1^+ marks the bottom of the valence bands. The way the energies of these points were derived from the data is illustrated in Fig. 10. The DOS of Asahina *et al.*[8] which reproduces the experimental *structures* in the valence bands best is broadened by folding it into a Gaussian of FWHM = 1.0 eV [Fig. 10(b)]. This width takes into account both the experimental resolution and approximately the lifetime broadening of the hole states. The broadened DOS and the valence-band spectrum resemble each other well enough to deduce "experimental" critical-point energies from a comparison of the two curves as indicated by the vertical lines in Fig. 10. The energies so obtained are listed

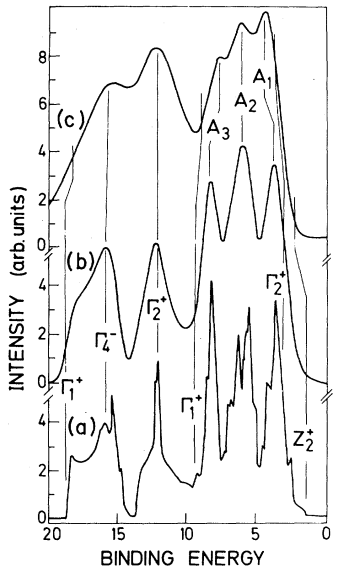

FIG. 10. Valence-band spectra of black phosphorus. (a) Density of states (DOS) as calculated by Asahina *et al.* (Ref. 8) using the pseudopotential method. (b) Calculated DOS broadened with Gaussian FWHM=1.0 eV. (c) XPS data with inelastic background subtracted (this work).

in Table IV together with the corresponding values from the band-structure calculations. The pseudopotential and to a lesser degree the tight-binding results are in fair agreement with experiment. Over all, the atomic-orbital-based scheme reported here, reproduces the experimental *results* best despite the fact that it contains no adjustable parameters.

B. White phosphorus

The valence-band spectrum of *w*-P is qualitatively different from those of the other P allotropes (Fig. 6). In fact, the white P spectrum is essentially the same as that of an isolated molecule. Nevertheless, the strong bulk and surface plasmons evident in Fig. 4 indicate that we are dealing with a molecular solid rather than a gas-phase spectrum.

The results of the molecular-orbital (MO) calculation of Table III for the P_4 molecule are compared with the valence-band spectrum of *w*-P in Fig. 11. To this end we weight the MO's according to their atomic-orbital character using the cross-section ratio. For Si, the element next to P, it has been determined that $\sigma(3s)/\sigma(3p)\simeq 3.4$.[37] Using the trend in this ratio with Z from calculations of Goldberg *et al.*,[38] we estimate a ratio $\sigma(3s)/\sigma(3p)\simeq 2.3$ for P. After a Gaussian broadening with FWHM=5.0, 3.0, and 1.5 eV is applied to the $4a_1$, $5t_2$, and ($5a_1$, $6t_2$, $2e$) states, respectively, the MO's give an excellent description of the *w*-P valence bands. The broadening takes into account the combined effect of the solid-state interaction of the P_4 molecules and finite lifetime of the MO's after photoexcitation. The four uppermost MO's are directly observed in uv photoemission from P_4 molecules.[35,39] Their binding energies are 9.6 ($2e$), 10.5 ($6t_2$), 11.9 ($5a_1$), and 15.8 eV ($5t_2$), respectively, measured relative to the vacuum level. Al$K\alpha$ photoemission spectra of P_4 molecules reveal peaks at 9.9 ($2e$, $6t_2$, and $5a_1$), 15.7 ($5t_2$) and 22.3 eV ($4a_1$) below the vacuum level.[40] Allowing for a 1-eV difference in the binding energy scale with respect to that of Fig. 11 these values are compatible with the position of the peaks in the spectrum of *w*-P, lending thus further support to the interpretation of the electronic structure of *w*-P in terms of weakly interacting P_4 tetrahedra.

C. Amorphous phosphorus

Band-structure calculations of amorphous phosphorus cannot be done because of the lack of crystal

TABLE IV. Energies (in eV) of critical points in the band structure of orthorhomic black phosphorus. Errors are given in parenthesis.

Critical point	Tight binding, Ref. 7	Pseudopotential, Ref. 8	Atomic-orbital, this work	Experiment, this work
Z_2^+	0	0	0	0
Γ_2^+	1.2	1.7	0.8	1.4(2)
Γ_4^+	1.7	3.7	2.2	
Γ_1^+	2.1	3.4	0.9	
Γ_3^-	2.3	4.3	6.1	
Γ_1^-	2.6	5.2	3.7	
Γ_4^-	3.8	5.4	2.3	
Γ_1^+	5.0	8.0	6.7	6.5(4)
Γ_2^+	7.1	10.5	9.8	9.6(2)
Γ_4^-	12.5	14.2	11.7	13.0(3)
Γ_1^+	16.6	17.0	14.6	15.6(5)

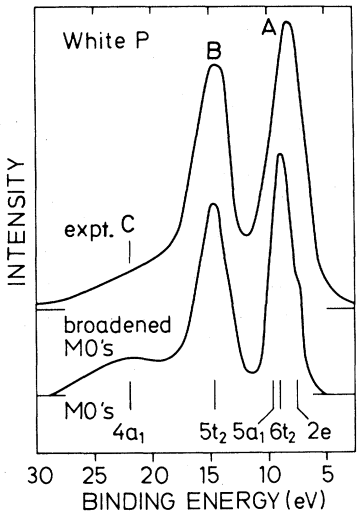

FIG. 11. Comparison of the measured and calculated electronic spectrum of w-P. The molecular orbitals (MO's) of a P_4 molecule have been weighted according to their atomic-orbital contribution and broadened with Gaussians as explained in the text.

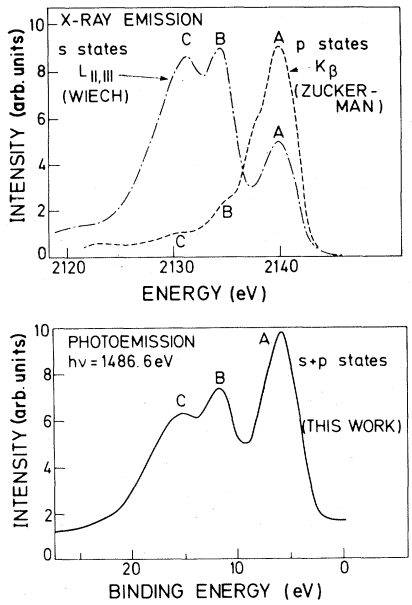

FIG. 12. Comparison of x-ray emission data of Wiech (Ref. 5) and Zuckerman (Ref. 6) with XPS data (this work) for bulk red amorphous phosphorus. The data have been scaled so that all spectra have equal maximum intensities.

structure. The valence-band spectra must therefore be interpreted by other means. They exhibit two regions of high intensity separated by a minimum. In analogy to the spectra of other group-V elements[9] and in comparison with the band-structure calculations described in the preceding section, we expect the top half to be due to P $3s$ electrons. This assignment is confirmed by a comparison of our XPS results with soft x-ray emission data obtained for r-P by Wiech[5] and Zuckerman[6] (see Fig. 12). Although not presented here, analogous data for b-P have been published by Wiech[5] and Fichter.[3] The dipole selection rules ensure that the $L_{\mathrm{II,III}}$ spectrum represents the $3s$ partial density of states (PDOS) and the K_β spectrum the $3p$ PDOS. Thus peak A is $3p$-like with some $3s$ hybridization and peaks B and C are $3s$-like with a lesser amount of $3p$ hybridization. In Fig. 12 all three spectra have been scaled to have an equal maximum height. The XPS spectrum represents the broadened valence-band DOS modulated by differences in the $3s$ and $3p$ cross sections. Using the ratio $\sigma(3s)/\sigma(3p)\simeq 2.3$ derived above for P yields a ratio of peak areas $(B+C)/A=1.5$ in fair agreement with the data.

The vibrational spectra (infrared and Raman) of red phosphorus and sputtered amorphous phosphorus have been interpreted in terms of the continuous-random-network (CRN) model for threefold-coordinated atoms.[31,41] The network was originally built to model the structure of amorphous arsenic (a-As) using pyramidal As_4 units.[42] In this way the nearest-neighbor configuration (coordination number, bond length, and bond angle) of the crystal (with rhombohedral $A7$ structure) is retained. Translational symmetry is lost by allowing free rotation about all bonds. The same model is, in principle, applicable to amorphous phosphorus since the nearest-neighbor configurations of P and As are the same aside from a slight difference in bond angle. The coordinates of the model were subsequently computer refined to minimize bond-length and bond-angle variation and the average bond angle could simultaneously be adjusted to values appropriate to a-As (98°) or a a-P (102°) employing the valence-force model of Keating to minimize local strain.[43]

The CRN model thus refined gives a good description of the radial distribution function (RDF) of a-As but the agreement with the RDF of r-P is only fair.[43] Calculations of the electronic structure[11] and of the vibrational spectra[44–46] of a-As based on the CRN model reproduce qualitatively the differences between the crystalline and amorphous data.[47–49]

Compared to a-As the infrared and Raman spectra of amorphous phosphorus in bulk and thin-film forms show considerably more structure which implies a higher degree of dynamical and structural order in amorphous P compared to a-As according to Lannin and co-workers.[31,41,50] Based on the presence of a strong (compared to a-As) low-angle dif-

fraction peak at $K \simeq 1.1$ Å^{-1} in a-P (bulk and thin film) they suggest that this order has the form of a layerlike structure with reduced interlayer coupling compared to the CRN model. Shanabrook and Lannin estimate a correlation length of this order of up to 29 Å from the width of the diffraction peak at 1.1 Å^{-1}, which corresponds to a real-space distance of 5.8 Å.[31] This is approximately the separation of the double layers in orthorhombic P whereas no corresponding set of planes exists in the rhombohedral structure.

The photoemission results of r-P and a-P:H are in substantial agreement with this structural model; the main difference between the crystalline and amorphous spectra, the 25% reduction in the width of the p-like peak (peak A in Fig. 6), is qualitatively reproduced by the theoretical density of states of a single layer of b-P [Fig. 9(b)]. The reduced width is due to the loss of interlayer interaction and indeed no such reduction is observed in the spectrum of a-As with its more three-dimensional structure.[9]

Furthermore, the bifurcation of the s-like peaks (B and C) in the valence bands of phosphorus are retained in the amorphous modifications whereas the corresponding dip is filled in the spectrum of a-As. Ley *et al.* suggested that this was due to the presence of odd-membered rings in the structure of a-As in analogy to the situation found in a-Si.[9] This view was subsequently corroborated by the model calculations of Kelly and Bullett[51] for a CRN model containing only even-membered rings and by the more general considerations of Robertson concerning the relationship between ring statistics and the shape of s bands in covalently bonded solids.[52] By the same token, the persistence of the dip in the s bands of a-P forces us to assume that the number of odd-membered rings is much reduced in a-P compared to a-As in agreement with the higher degree of intralayer order in a-P. The orthorhombic double layers contain only six-numbered rings, whereas the CRN model of Greaves and Davis has about equal numbers of five- and sixfold rings.[42]

This line of reasoning is disturbed, however, by the spectra of NaP_{15} (Fig. 7). There is a close resemblance between the valence bands of NaP_{15} and those of r-P and a-P:H. The width of peak A is the same in all three spectra if we disregard the shoulder $A2$ for the time being. The bifurcation of the s-like peaks is present in NaP_{15} despite the fact that the phosphorus tubes contain three times as many fivefold as sixfold rings. It appears therefore that the original suggestion of Thurn and Krebs[25] that r-P contains the same structural units as Hittorf's phosphorus, namely pentagonal tubes of phosphorus, can no longer be dismissed. This suggestion was based on the similarity of the RDF's of the two materials, in particular for those distances present *within* the tubes whereas differences occurred for the distances *between* neighboring tubes. The valence-band spectra of amorphous P may thus well represent the local density of these tubes since they occur with little variation also in NaP_{15}, and P—P bonds between the tubes are responsible for the shoulder $A2$. The presence of a diffraction peak at $k \simeq 1.1$ Å^{-1} is no obstacle to this interpretation since Vepřek and Beyder have shown that this maximum cannot be simply interpreted in terms of a coherence distance in real space.[53] They surmise that the peak is instead related to clustering in the morphology of amorphous materials.

In view of the results presented here it appears worthwhile to measure Raman and infrared spectra of Hittorf's phosphorus as an additional means to distinguish between the two fundamentally different models for the structure of amorphous phosphorus. The valence-band spectra of NaP_{15} raise the additional question why the connection between ring statistics and the shape of the s bands as discussed by Robertson[50] does not hold for the pentagonal tubes in phosphorus.

VI. SUMMARY

We have presented x-ray photoemission spectra (XPS) for four allotropes of phosphorus and for NaP_{15} and compared them with calculations and other measurements from the literature wherever possible. This included the three most common bulk modifications, i.e., black orthorhombic phosphorus (b-P) white phosphorus (w-P) and bulk amorphous red phosphorus (r-P), as well as a new material, glow-discharge-deposited hydrogenated amorphous thin-film phosphorus (a-P:H). NaP_{15} contains structural elements (pentagonal tubes of P atoms) which occur also in Hittorf's phosphorus, another crystalline allotrope of P.

The core-line positions are independent of allotrope although the line shapes vary a little. The spin-orbit splitting visible for b-P is smeared out due to differential charging in the more resistive samples. The plasmon energies, which in the free-electron approximation are proportional to the square root of the density of valence electrons, are consistent with variations in the density of the samples.

In spite of these similarities, there are significant differences among the valence-band structures of the various modifications, indicating differences in the nature of the bonding. The valence band of w-P contains two isolated peaks which can be understood in the context of our molecular-orbital calculations for P_4 molecules. This finding is in agreement with the lack of interaction among the tetrahedral P_4

units comprising *w*-P as evidenced by the high volatility and instability of *w*-P.

Results for *b*-P are in excellent agreement with band-structure calculations. There is a three-component *p*-type and a two-component *s*-type band. The *s*-type band is essentially the same in *r*-P and *a*-P:H as in *b*-P, as expected since the *s* electrons contribute very little to the bonding. The threefold structure of the *p*-type band, however, is observed only for *b*-P. This band is considerably narrower for both *r*-P and *a*-P:H.

The differences in the valence bands between *b*-P and the amorphous modifications are equally well explained by model structures consisting of weakly interacting phosphorus double layers as they occur in *b*-P and by the pentagonal tubes that are characteristic for NaP_{15} and Hittorf's phosphorus. It is suggested that additional measurements on these forms of phosphorus are performed to gain more insight into the intermediate-range order present in amorphous phosphorus.

ACKNOWLEDGMENTS

We are extremely grateful to Dr. H. Richter for helpful discussions and assistance in many phases of this work. The invaluable technical assistance of W. Neu is also deeply appreciated. We thank Professor J. S. Lannin for providing the black and red phosphorus samples, Professor H. G. von Schnering, Dr. R. Santandrea, and Dr. W. Hönle for the NaP_{15} sample and for a number of useful discussions, and Dr. Hideo Asahina for sending us copies of papers prior to publication. One of us (N.B.G.) is supported in part by a North Atlantic Treaty Organization fellowship.

*Present address: Xerox Webster Research Center, 800 Phillips Road, Webster, New York, 14580.

†Permanent address: School of Physics, University of Bath, Bath BA2 7AY, Great Britain.

[1]D. E. C. Corbridge, *Phosphorus: An Outline of its Chemistry Biochemistry and Technology* (Elsevier, Amsterdam, 1978), p. 1.

[2]D. E. C. Corbridge, *The Structural Chemistry of Phosphorus* (Elsevier, Amsterdam, 1974), p. 13.

[3]M. Fichter, Ph.D. dissertation, Universität München, 1966 (unpublished).

[4]V. A. Fomichev, Fiz. Tverd. Tela 9, 3034 (1967) [Sov. Phys.—Solid State, 9, 2398 (1968)].

[5]G. Wiech, Z. Phys. 216, 472 (1968).

[6]S. Zuckerman, Ph.D. thesis, Université Pierre et Marie Curie, Paris VI, France 1981 (unpublished).

[7]Y. Takao, H. Asahina, and A. Morita, J. Phys. Soc. Jpn. 50, 3362 (1981); Y. Takao and A. Morita, Physica 105B, 93 (1981).

[8]H. Asahina, K. Shindo, and A. Morita, J. Phys. Soc. Jpn. 51, 1193 (1982); H. Asahina, A. Morita, and K. Shindo, J. Phys. Soc. Jpn. 49, Suppl. A, 85 (1980).

[9]L. Ley, R. A. Pollak, S. P. Kowalczyk, R. McFeely, and D. A. Shirley, Phys. Rev. B 8, 641 (1973).

[10]D. W. Bullett, Solid State Commun. 17, 965 (1975).

[11]M. J. Kelly and D. W. Bullett, Solid State Commun. 18, 593 (1976).

[12]D. W. Bullett, Philos. Mag. 36, 1529 (1977).

[13]L. M. Falicov and S. Golin, Phys. Rev. 137, A871 (1965).

[14]S. Golin, Phys. Rev. 140, A993 (1965).

[15]L. M. Falicov and P. J. Lin, Phys. Rev. 141, 562 (1966).

[16]S. Golin, Phys. Rev. 166, 643 (1968).

[17]B. von Roedern, L. Ley, M. Cardona, F. W. Smith, Philos. Mag. 40, 433 (1979).

[18]H. Krebs and H. U. Gruber, Z. Naturforschg. 22a, 96 (1967).

[19]P. W. Bridgeman, J. Am. Chem. Soc. 36, 1344 (1914).

[20]A. Brown and St. Rundquist, Acta Crystallogr. 19, 684 (1965).

[21]R. W. Keyes, Phys. Rev. 92, 580 (1953).

[22]D. Warschauer, J. Appl. Phys. 34, 1853 (1963).

[23]Y. Maruyama, S. Suzuki, K. Kobayashi, and S. Tanuma, Physica 105B, 99 (1981).

[24]W. Hittorf, Ann. Phys. Chem. 126, 193, 215 (1865).

[25]H. Thurn and H. Krebs, Acta Crystallogr. B 25, 125 (1969).

[26]H. G. von Schnering, in *Homoatomic Rings, Chains, and Macromolecules,* edited by A. L. Rheingold (Elsevier, New York, 1977), Chap. 15.

[27]W. Wichelhaus, Ph.D. thesis, Universität Münster, 1975 (unpublished).

[28]T. S. Moss, *Photoconductivity in the Elements* (Butterworths, London, 1952), p. 141.

[29]S. Vepřek and H. R. Oswald, Z. Anorg. Allg. Chem. 412, 190 (1975).

[30]J. Brunner, M. Thuler, S. Vepřek, and R. Wild, J. Phys. Chem. Solids 40, 967 (1979).

[31]B. V. Shanabrook and J. S. Lannin, Phys. Rev. B 24, 4771 (1981).

[32]J. Schilling, Z. Phys. B 25, 61 (1976).

[33]Y. Harada, K. Murano, I. Shirotani, T. Takahashi, and Y. Maruyama, Solid State Commun. 44, 877 (1982).

[34]J. H. Scofield, J. Electron. Spectrosc. Relat. Phenom. 8, 129 (1976).

[35]C. R. Brundle, N. A. Kübler, M. B. Robin, and H. Basch, Inorg. Chem. 11, 20 (1972).

[36]G. Seifert and G. Grossmann, Z. Anorg. Allg. Chem. 18, 233 (1978).

[37]R. G. Cavell, S. P. Kowalczyk, L. Ley, R. A. Pollak, B.

Mills, D. A. Shirley, and W. Perry, Phys. Rev. B 7, 5313 (1973).
[38]S. M. Goldberg, C. S. Fadley, and S. Kono, J. Electron. Spectrosc. Relat. Phenom. 21, 285 (1981).
[39]S. Evans, P. J. Joachim, A. F. Orchard, and D. W. Turner, Int. J. Mass Spectrom. Ion Phys. 9, 41 (1972).
[40]M. S. Banna, D. C. Frost, C. A. McDowell, and B. Wallbank, J. Chem. Phys. 66, 3509 (1977).
[41]B. V. Shanabrook, J. S. Lannin, and P. C. Taylor, Solid State Commun. 32, 1279 (1979).
[42]G. N. Greaves and E. A. Davis, Philos. Mag. 29, 1201 (1974).
[43]E. A. Davis, S. R. Elliot, G. N. Greaves, and P. D. Jones, in *The Structure of Non-Crystalline Materials,* edited by P. H. Gaskell (Taylor and Francis, London, 1977), p. 205.
[44]P. E. Meek, in Ref. 41, p. 235.
[45]D. Beeman and R. Alben, Adv. Phys. 26, 339 (1977).
[46]W. Pollard and J. D. Joannopoulos, Phys. Rev. B 21, 760 (1980).
[47]A. J. Leadbetter, P. H. Smith, and P. Seyfert, Philos. Mag. 33, 441 (1976).
[48]G. Lucovsky and J. C. Knights, Phys. Rev. B 10, 4324 (1974).
[49]J. S. Lannin, Phys. Rev. B 15, 3863 (1977).
[50]J. S. Lannin and B. V. Shanabrook, Solid State Commun. 28, 497 (1978).
[51]M. J. Kelly and D. W. Bullett, Philos. Mag. B 38, 423 (1978).
[52]J. Robertson, J. Phys. C 8, 3131 (1975).
[53]S. Vepřek and H. U. Beyder, Philos. Mag. B 44, 557 (1981).